NORMALISATION OF LOAD AND CLEARANCE EFFECTS IN BALL IN SOCKET-LIKE REPLACEMENTS

Ciavarella[*], M., Strozzi[^], A., Baldini[^], A., Giacopini[^], M.

[*]CEMEC-PoliBA, Bari, Italy

[^]University of Modena and Reggio Emilia, Italy

Abstract

A normalising loading parameter useful in summarising the mechanical response of plane, pin in plate-like contacts is extended to axisymmetric, ball in socket-like contacts. Various diagrams reporting mechanically relevant dry frictionless contact parameters versus the loading parameter in compliant layered artificial hip joints and in metal-on-metal hip replacements are presented and assessed versus several literature results, Finally, the usefulness of the normalising loading parameter is expounded.

Keywords: compliant layered hip replacement, metal-on-metal hip replacement, contact problem, clearance effects, normalisation, loading parameter.

1 Introduction

The contact between a sphere and a spherical cavity in the presence of an initial clearance is classified as a progressive contact, since the contact area increases with load, *e.g.* Dundurs and Stippes [**1**]. Consequently, such a contact problem is nonlinear, and nonlinearity makes it difficult to normalise its mechanical response with respect to the initial gap and applied load effects for a general configuration.

Ciavarella *et al.* [**2**] have recently defined a loading parameter normalising the nonlinear effects of load and clearance for plane, pin in plate-like problems. A brief historical review of pioneering developments of a normalising loading parameter is presented in [**3**], to which the interested reader is referred. An extension of the normalising loading parameter to axisymmetric, ball in socket-type problems is proposed in this work, having in mind stress analysis problems encountered in hip replacements.

The outline of this paper is as follows. Section 2 presents a simple graphical explanation of the loading parameter concept applied to axisymmetric ball in socket-type problems. Section 3 addresses the application of the loading parameter to soft cushion-type hip replacements for a range of soft layer thicknesses. Various comparisons with literature results are presented, and the merits of this normalising approach are expounded. Finally, Section 4 reports a preliminary study of metal-on-metal hip replacements, interpreted in the light of the loading parameter.

2 The normalising loading parameter Φ in ball in socket-like contacts

The grouping of variables defining the correct loading parameter Φ for axisymmetric geometries in frictionless, closely conforming, ball in socket-type progressive contacts, is here determined by essentially resorting to graphical explanations rather than to formal mathematics, in order to render this treatment accessible to non specialists. (A formal approach could be developed by following the same guidelines of Ciavarella *et al.* [**2**].)

In the interest of simplicity, in the following explanation the assumption is made that the socket is deformable whereas the indenting sphere is rigid. The proposed graphical interpretation is based upon four points; the first point considers only the socket and ignores the presence of the ball; the remaining points gradually include various aspects of the contact problem between ball and socket. More precisely, the four points are: 1) analysis of the effects of dimensions and pressure intensity on the socket deformability, see Figure 1; 2) determination of the variation of the clearance profile between ball and socket for a generic angular position when the initial clearance is altered with respect to a reference situation, see Figure 2; 3) examination of the role of the Young's modulus in contact problems, see equation (4); 4) evaluation, based on the results already achieved in 1), of the variation of the socket deformability as a result of a change of the contact pressure or of the socket dimensions and, above all, determination of the alteration of the sphere dimension that renders the sphere consistent with the two above socket modifications, see Figure 3. These four points are discussed in more detail below.

1) Some simple observations are presented with regard to the deformability of an axisymmetric body, having in mind ball in socket-like contact problems. In particular, the deformability of the socket as a result of an imposed pressure profile is explored when a) the socket shape and dimensions are kept equal whereas the imposed pressure is doubled with respect to a reference situation; b) the socket shape and imposed pressure profile are kept fixed, whereas the socket dimensions are doubled.
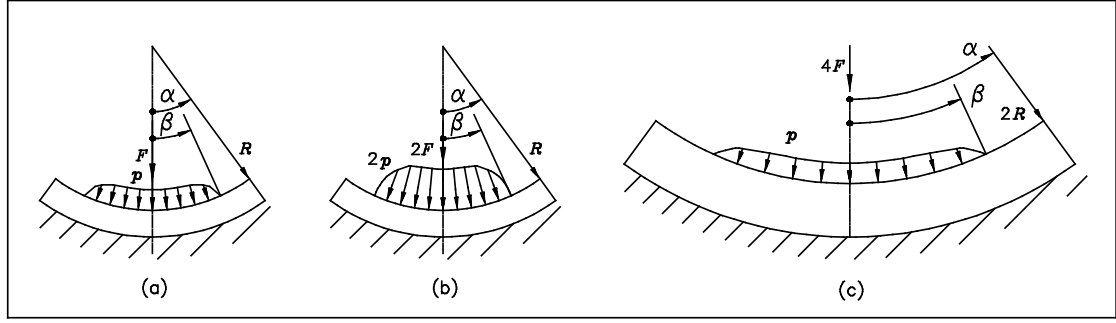
Figure 1

Figure 1 (a) presents a deformable axisymmetric socket of inner radius R and angular extent α, loaded by an axisymmetrically distributed pressure p acting within a region defined by the angle β, firmly bonded to a rigid substrate along its lower surface. (In the interest of simplicity, in Figure 1 only a meridional cross section of the cup is represented.) The vertical resultant of the pressure distribution is named F. This pressure profile causes deflections of the socket loaded face which are inversely proportional to the socket Young's modulus E. Figure 1 (b) displays an equal cup loaded by a doubled pressure profile $2p$ acting on the same circular region. The resultant of the pressure distribution is therefore $2F$, and the deflection of the cup loaded surface is doubled with respect to that of Figure 2 (a). Finally, Figure 1 (c) shows a cup of the same shape but of doubled dimensions with respect to Figure 1 (a). The inner radius thus becomes $2R$, the cup radial thickness is doubled, whereas the cup angular extent α remains unaltered. This cup is loaded by a pressure p acting within an axisymmetric zone defined by the same angle β. This pressure profile and its maximum value are unaltered with respect to Figure 1 (a). The resultant of the pressure distribution is $4F$, whereas the cup deflections are only doubled with respect to those of Figure 1 (a), *e.g.* Johnson [4], p. 56.

2) Some observations are presented in the following with regard to the initial clearance between ball and socket. In particular, the variation of the clearance profile between ball and socket for a generic angular position is examined when the initial radial clearance is doubled with respect to a reference situation. Figure 2 (a) shows a meridional cross section of a ball in socket-like contact problem, which evidences the initial gap δ between sphere and spherical cavity as a function of the angular coordinate ϑ, due to an

initial radial clearance ΔR. (In the interest of clarity, an unrealistically large clearance has been represented in Figure 2.) The classical approximation of the initial gap valid for closely conforming contacts is, *e.g.* Ciavarella and Decuzzi [5]:

$$\delta(\vartheta) = \Delta R(1 - cos\vartheta) \tag{1}$$

This description of the initial gap is very accurate for any angular coordinate ϑ for realistic initial clearances. Therefore, contrary to a Hertzian-type approach, the results of this study remain accurate even in the situation of large contact zones.

Figure 2 (b) shows the initial gap δ versus the angular coordinate ϑ in the presence of a doubled initial radial clearance $2\Delta R$. The initial gap becomes:

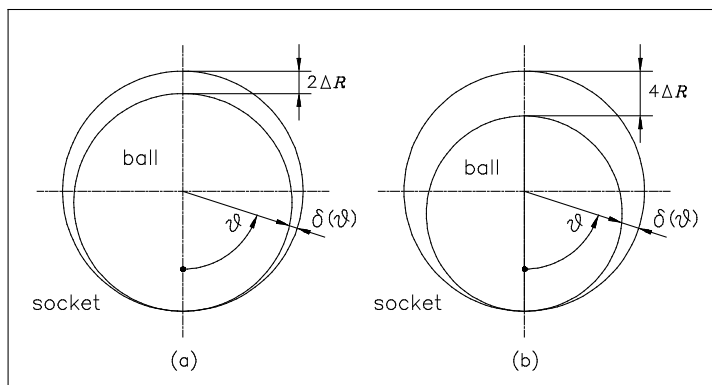$$\delta(\vartheta) = 2\Delta R(1 - cos\vartheta) \tag{2}$$

Figure 2

It is clearly seen that, if the initial radial clearance is doubled, the initial gap is also doubled for any angular position ϑ. In other words, since in (2) the term $(1-cos\vartheta)$ of the initial gap expression remains unaltered with respect to (1), the distribution of δ in the θ direction remains unchanged.

It is noted at this stage that the above property of the approximate expression of the initial clearance is absent in the exact expression, which exhibits a nonlinear character with respect to the initial radial clearance, *e.g.* formula (46) of Strozzi [6]. As a consequence of nonlinearity, in the exact expression the gap profile would be (slightly) altered by a change in the initial clearance.

Since the loading parameter Φ is based upon the approximation (1), the contacting surfaces must be closely conforming.

3) The following observations address the role of the Young's modulus in contact problems where the two contacting bodies are
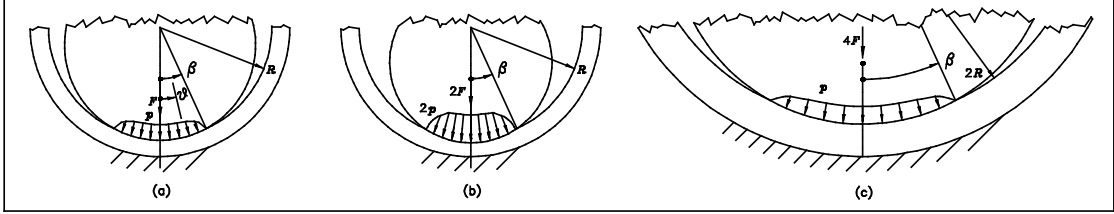

Figure 3

made of the same material, or when one of the bodies is rigid. Figure 3 (a) illustrates a meridional cross section of a ball in socket-like contact problem in the deformed configuration. The correct contact pressure distribution p activated by the contact force F within the contact region is the pressure profile that produces deflections of ball and socket capable of annulling the initial clearance δ within the whole embedding region defined by the angle β. The contact pressure will therefore be the solution of an integral equation of the form:

$$\int_0^\beta p(\omega)k(\vartheta,\omega)Rd\omega = \delta(\vartheta) \tag{3}$$

where the angle β defines the contact region, R is the curvature radius of the two mating surfaces before deformation, ϑ is the angular coordinate, ω is a dummy variable, and k is the kernel constituting the influence function that expresses the combined deformability of socket and sphere. (Since ΔR is small, R defines the radius of curvature of both socket inner surface and sphere surface.) Limiting ourselves to the situation in which the two contacting bodies exhibit the same Young's modulus E, or to the case in which one of the contacting bodies is rigid, the kernel k is inversely proportional to E, so that equation (3) may be rewritten as:

$$\int_0^\beta p(\omega)\frac{\overline{k}(\vartheta,\omega)}{E}Rd\omega = \delta(\vartheta) \Rightarrow \int_0^\beta p(\omega)\overline{k}(\vartheta,\omega)Rd\omega = E\delta(\vartheta) \tag{4}$$

6

where $\bar{k}$ is an influence function computed for $E=1$, that is, normalised with respect to E. Equation (4) shows that the grouping of variables $E\,\delta$ — in the following the grouping $E\Delta R$ will be employed — normalises the Young's modulus effects.

4) Some observations on the correct distribution of the contact pressure are developed in the following. These observations rely mainly upon the results already obtained in point 1). As in Figure 1, the socket deformability as a result of the sphere indentation is explored when a) the socket shape and dimensions are kept equal whereas the contact pressure is doubled with respect to a reference situation; b) the socket shape and contact pressure profile are kept constant, whereas the socket dimensions are doubled. The main aim is to clarify which alterations of the sphere dimension are consistent with the two socket modifications a) and b).

Figure 3 (a) illustrates a meridional cross section of a ball in socket-like contact problem in the deformed configuration. As already observed, the correct contact pressure distribution p originated by the contact force F within the contact region is the pressure profile that produces deflections of ball and socked capable of annulling the initial clearance δ within the whole embedding region defined by the angle β. In Figure 3 (b) the same dimensions are considered for ball and socket and for the angular extent β of the contact zone; the contact pressure is assumed to be doubled with respect to Figure 3 (a), which implies that the total load F is doubled. (In Figure 3 (b) the ball diameter is perceivably smaller than that of Figure 3 (a). This is due to the circumstance that, in the interest of clarity, a high value of the initial radial clearance ΔR has been adopted. If a value of ΔR in the region of a fraction of a millimetre had been employed, the difference in diameter of the spheres of Figures 3 (a) and (b) would have been hardly appreciable.) According to the comments referring to Figure 1 (b), the deflections of the mating surfaces of ball and socket will be doubled. Taking account of the comments to equation (3) and to Figure 2 (b), the spherical cavity in the socket due to the doubled deflections may be interpreted to have been caused by an indentation of a sphere whose diameter is consistent with a doubling of the initial radial clearance ΔR. Consequently, for fixed shape and dimensions of a ball in socket-like contact problem, the parameter $F/(E\Delta R)$ is an indicator of the contact extent and of the stress

concentration-like parameters (*e.g.* the peak contact pressure normalised with respect to the a proper reference contact pressure). It may be concluded that, for fixed shape and dimensions this parameter summarises the initial clearance, total load and Young's modulus effects on the dry contact stress parameters.

The above parameter, valid for axisymmetric contact problems, is formally equal to its analogue in plane contacts, Ciavarella *et al.* [**2**]. In plane contacts *F* represents a force per unit thickness, whereas in axisymmetric contacts *F* indicates the total load. Consequently, in axisymmetric contact problems the above parameter is dimensional — its dimension is a length — and, therefore, it is not suitable for describing a class of axisymmetric contact problems exhibiting the same shape but different dimensions. To overcome this problem, it is necessary to introduce a term expressing a length at the denominator of the above grouping of variables, as noted in Ciavarella *et al.* [**2**]. The observations which follow determine the correct variable to be added to the above factor.

In Figure 3 (c) the same shape but doubled values are considered for the dimensions of ball and socket. The inner radius thus becomes $2R$. The contact pressure *p* acts within an axisymmetric zone defined by the same angle β. The pressure profile and its maximum value are unaltered with respect to Figure 3 (a). This implies that the total load *F* becomes four times as much, whereas the ball and socket deflections are only doubled with respect to those of Figure 3 (a) (see the comments referring to Figure 1 (c)). The doubling of deflections indicates that this contact problem is consistent with a doubling of the initial radial clearance Δ*R,* as already commented. It is also evident that the grouping of variables $\Phi = F/(ER\Delta R)$, where *R* is the curvature radius of the mating surfaces before deformation, remains unaltered for the cases of Figure 3 (a) and (c). In fact, passing from Figure 3 (a) to (c), *F* is quadrupled, whereas both *R* and Δ*R* are doubled. Consequently, the above loading parameter Φ remains constant for a whole class of ball in socket-like axisymmetric contact problems for which the geometry is the same but the dimensions are varied, and for which the combination of total load *F* and initial radial clearance Δ*R* produce the same angular extent of the contact zone. Therefore, for a specific ball in socket-like geometry but for general dimensions, initial clearance, total load and Young's modulus, it is possible to

compile diagrams reporting along the *x*-axis the loading parameter Φ and along the *y*-axis the normalised peak dry contact problem, the normalised shear stress at the interface between cup and support, the angular extent β of the contact zone, and so on.

It is finally noted that for the axisymmetric contact of a sphere inside a complete spherical cavity ($\alpha=\pi$ in Figure 1 (a)), the same asymptotic conclusions valid for the corresponding plane contact, Ciavarella *et al.* [2], hold true. In particular, as the load is increased in the presence of an initial clearance, both the stress concentration factor and the contact arc extent approach the corresponding values referring to a neat fit. It is expected that this result approximately holds even if the spherical cavity is not complete, for example if the socket is hemispherical, as it occurs in practical applications.

3 Application of the loading parameter Φ to soft cushion hip replacements

The prospect of replacing arthritic joints with replacements that mimic the natural lubrication mechanism was suggested in 1981 by Unsworth *et al.* [**7**]. The principle is that a soft elastomeric layer is attached to a harder backing material to simulate cartilage on bone.

A variety of studies are available in which the effects are addressed of modifications in layer thickness, initial clearance, applied load, and elastic constants, on the mechanical response of joints whose cup is covered with a deformable layer, *e.g.* Bartel *et al.* [**8**] (referring to a metal-backed plastic layer), Unsworth *et al.* [**9**] (referring to softer layers), Strozzi [**10**] (which contains a thorough literature review on contact stresses in soft cushion hip replacements up to 1992), Strozzi and Unsworth [**11**], Jin *et al.* [**12**], Yao *et al.* [**13**], Unsworth and Strozzi [**14**], Strozzi [**6**], Jin [**15**], Wang *et al.* [**16**]. In such studies the effects of variations of the above-listed parameters have been examined individually, so that an extensive parametric analysis had to be undertaken, and the relevant mechanical information was inevitably scattered throughout several design charts. For instance, in Strozzi and Unsworth [**11**] and in Unsworth and Strozzi [**14**], four basic configurations of a soft-layered joint were examined, and two major separate sensitivity analyses were carried out with regard to layer thickness and initial clearance. In Jin *et al.* [**12**] an extensive parametric stress analysis was undertaken, where the parameters investigated independently included the radius of the femoral head, the radial clearance, the elastic modulus, and the layer thickness. In Yao *et al.* [**13**] the separate effects of initial clearance, material, and layer thickness on the maximum interface shear stress and on the contact extent were investigated. Finally, in Wang *et al.* [**16**] a thorough parametric appraisal of a perturbation of the initial clearance was carried out.

The loading parameter Φ may conveniently summarise the interrelated effects of initial clearance, applied load, head diameter, and Young's modulus, on the dry contact stress parameters in soft cushion hip replacements. In particular, condensed diagrams can promptly be compiled in which various relevant stress parameters are reported versus the unifying loading parameter Φ. A very limited number of curves can therefore embody a comprehensive and

systematised account of the combined effects of clearance, load, head diameter, and Young's modulus, on normalised peak contact pressure, normalised maximum interface shear strain between layer and backing, contact angle, and angle defining the position of the maximum interface shear stress. Such curves are presented in this paper in Figures 4 to 7. Since Φ cannot normalise the layer thickness effects, each diagram curve is valid for a specific layer inner to outer radii ratio.

The diagrams presented in this work refer to a deformable layer possessing a perfectly hemispherical geometry, and being firmly bonded to a rigid substrate and compressed by a rigid head. Although during walking the force applied to the sphere deviates from the direction of the socket symmetry axis, by adopting a usual simplifying assumption this force is here considered as axial. Finally, due to the presence of the synovial fluid, the head-layer dry contact is considered as frictionless.

The essentials of the soft cushion hip replacement are illustrated in the insets of Figures 4 to 7, which clarify the meaning of the main symbols adopted. In particular, the radius R employed in the definition of the loading parameter Φ has been chosen to be the inner radius of the deformable layer. The load applied to the head is denoted by F.

To compile the diagrams reporting the above listed dry contact stress parameters versus Φ, it is convenient to refer to specific dimensions for the hip replacement, and to alter one of the parameters defining Φ, so that a wide Φ interval is explored. In a finite element analysis it is particularly convenient to vary the applied load F.

The following dimensions for the elastomeric layer have been extracted from Strozzi and Unsworth [11]: the layer inner radius r_i is 16.125 mm; the radial clearance ΔR is 0.25 mm, so that the head radius is 15.875 mm; four values of the layer outer radius r_o have been considered, namely 16.625 , 17.125 , 18.125 , 19.125 mm, so that the four layer thicknesses are 0.5 , 1 , 2 , 3 mm, and the four inner to outer radii ratios r_i/r_o are 0.9699 , 0.9416 , 0.8897 , 0.8431. The Young's modulus is 8.506 MPa, and the Poisson's ratio is 0.49942. A neo-Hookean constitutive relationship has been employed, *e.g.* Prati and Strozzi [17].
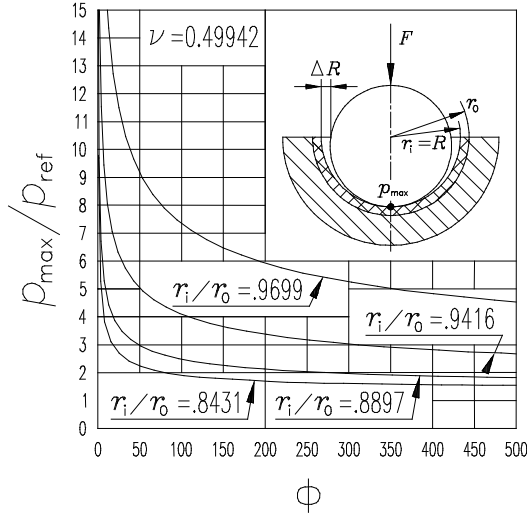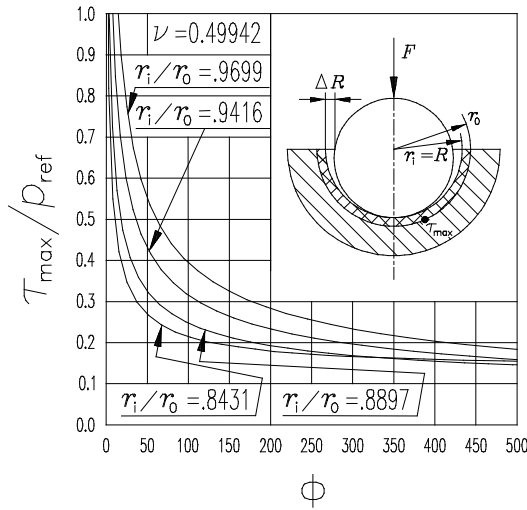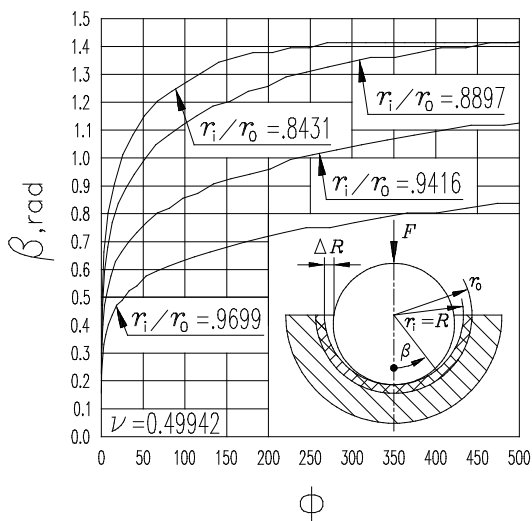
Figure 4

Figure 5

Figure 6

Several finite element calculations have been performed with the commercial package MSC Marc 2005, and the stress field has been expressed in terms of Cauchy stresses. The above layer dimensions, initial clearance and material constants have been adopted, and a load ramp from 0 to about 13 kN has been imposed. (Higher values of the load produced noticeable distortions within the elastomeric layer and caused convergence difficulties.)

For each load value, the loading parameter Φ has been reported along the x-axis of the diagrams of Figures 4 to 7, and the following four mechanically relevant parameters have been reported along the y-axis of the four diagrams: a) the peak dry frictionless contact pressure p_{max} normalised over the reference contact pressure p_{ref}, defined as $F/(\pi R^2)$, where F is the total load and R is the inner radius of the layer, see Figure 4; b) the maximum interfacial shear stress τ_{max} between layer and backing, normalised over p_{ref}, see Figure 5; c) the contact angle β expressed in radians, see Figure 6; d) the angle γ defining the position of the maximum interfacial shear stress, expressed in radians, see Figure 7. Every diagram includes four curves, each referring to one of the four above detailed layer outer to inner radii ratios.

12

The range adopted for Φ covers extreme situations of low load or of large initial clearance (low Φ values) and of high load or of small initial clearance (high Φ values).

The normalising capabilities of the loading parameter Φ clearly emerge from the following observation. Although the above curves have been derived for specific head and layer dimensions, initial clearance and Young's modulus, they describe the main mechanical features of the dry contact stress for any hollow hemispherical layer shape defined by one of the four inner to outer radii ratios 0.9699 , 0.9416 , 0.8897 , 0.8431 , and by any head radius, initial radial clearance, applied load and Young's modulus. An example is reported in detail at the end of this Section, which shows that the four diagrams of Figures 4 to 7 can be employed for examining the mechanical response of hip replacements exhibiting dimensions, initial clearance, and applied load completely different from those adopted in the compilation of the diagrams.
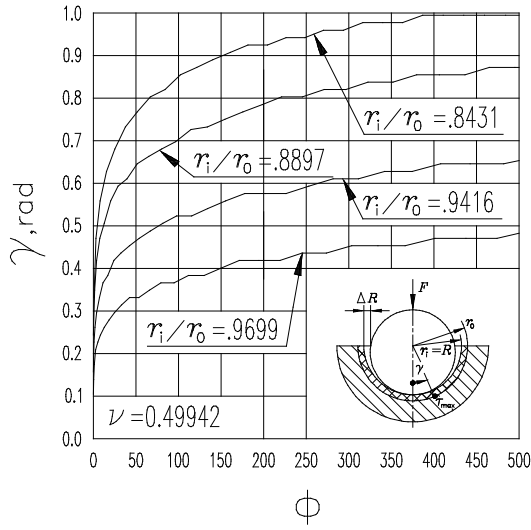

Figure 7

Instead, the above diagrams are theoretically inapplicable if the Poisson's ratio differs from the figure employed in the finite element study. It is, however, observed that in soft cushion hip replacements, in which the load (and not the indentation depth) is imposed, the numerical forecasts of Unsworth and Strozzi [**14**] show a weak dependence of the mechanical response of the replacement on the Poisson's ratio in the vicinity of the incompressibility value. It may therefore be concluded that the above diagrams are technically applicable when the Poisson's ratio is sufficiently close to the incompressibility value 0.5, although it would be difficult to define the validity range of this assumption.

It may additionally be observed that the finite element packages, when involving a contact problem, adopt the finite elasticity theory, whereas the loading parameter Φ holds in linear elasticity. Consequently, the validity of the diagrams of Figure 4 to

13

7, based upon both the finite element predictions and the loading parameter normalisation, may be questionable. However, it has numerically been shown by Strozzi and Unsworth [18] that the finite elasticity effects are negligible in this kind of contact problems.

It is also noted that the loading parameter Φ refers to dry contacts, and it cannot incorporate the lubrication effects. It is, however, known that in soft contacts the dry and lubricated pressure profiles are very similar, *e.g.* Strozzi and Unsworth [11].

Selected comparisons between the numerical forecasts of Figures 4 to 7 and various literature results are presented in the following. Comparisons are carried out between the peak contact pressure reported in Figure 3 of Strozzi and Unsworth [11] and Figure 4 of this work, between the maximum interface shear stress of Figure 3 of [11] and Figure 5 of this work, between the contact angle of Figure 4 of [11] and Figure 6 of this work and, finally, between the angle defining the position of the maximum interfacial shear stress, extracted from Figure 4 of [11], and Figure 7 of this work.

The considered layer inner and outer radii are 16.125 and 16.625 mm, respectively; the initial radial clearance is 0.25 mm and the Young's modulus is 8.506 MPa. For an indentation depth of 35 μm, Figure 2 of [11] indicates a load of 4000 N, Figure 3 of [11] displays a peak contact pressure of 34 MPa and a maximum interface shear stress of 2 MPa, whereas Figure 4 of [11] shows a contact angle of 0.65 rad and an angle defining the position of the maximum interfacial shear stress of 0.39 rad.

Since the reference pressure p_{ref} is $4000/(\pi \times 16.125^2) = 4.90$ MPa, the normalised peak contact pressure is $34/4.90 = 6.94$, whilst the normalised maximum interface shear stress is $2/4.90 = 0.41$.

The loading parameter Φ is $4000/(8.506 \times 16.125 \times 0.25) = 116.65$. From Figure 4 of this paper the normalised peak contact pressure referring to $\Phi = 116.65$ and to $r_{\text{i}}/r_{\text{o}} = 16.125/16.625 = 0.9699$ is about 7; from Figure 5 the normalised maximum interface shear stress is about 0.37; from Figure 6 the contact angle is 0.65; from Figure 7 the angle defining the position of the maximum interfacial shear stress is 0.38 .

The above numerical comparisons indicate that the forecasts extracted from Figures 4 to 7 closely agree with the numerical predictions of Strozzi and Unsworth [11]. In particular, the

maximum interface shear stress has been confirmed to be of the order of one tenth the peak contact pressure. It is, however, observed that, although Figures 4 to 7 of this paper summarise all the stress oriented diagrams of Strozzi and Unsworth [11] and of Unsworth and Strozzi [14], they cannot substitute the diagrams addressing the indentation depth, available in the above quoted papers.

A comparison between the peak contact pressure reported in Figure 7 (a) of Bartel et $al.$ [8] and Figure 4 of this work is carried out in the following. A head radius of 14 mm, a layer inner radius of 14.05 mm, a layer thickness of 2.615 mm, a Young's modulus of 1400 MPa, and a force of 2100 N are considered. The initial radial clearance is therefore 0.05 mm. The value of r_i/r_o is 14.05/(14.05+2.615) = 0.8431 . From Figure 7 (a) of Bartel et $al.$ [8] the peak contact pressure is about 18 MPa. In addition, p_{ref} = 2100/($\pi \times 14.05^2$) = 3.39 MPa, so that the normalised peak contact pressure is 18/3.39 = 5.32 . The loading parameter Φ is 2100/(1400×14.05× 0.05) = 2.135 . For the above Φ value and for r_i/r_o = 0.8431 , diagram 4 of this paper indicates a normalised peak contact pressure of about 6, which reasonably agrees with the value 5.32 of Bartel et $al.$ [8], the error being about 13 per cent.

It is frankly admitted that it is difficult to extract the above finite element prediction of the normalised peak contact pressure from the diagram Figure 4, as a result of the high gradients occurring for low Φ values. In fact, the diagrams of this study have been conceived for elastomeric materials exhibiting Young's moduli lower that those encountered in the study of Bartel et $al.$ [8], addressing a metal-backed plastic layer. The application of diagrams based upon the Φ parameter to relatively high Young's moduli would require the compilation of diagrams particularly focused upon low Φ values.

It is also observed that, while Figures 4 to 7 refer to almost incompressible elastomers characterised by a Poisson's ratio of nearly 0.5, the plastic material employed by Bartel et $al.$ [8] exhibits ν = 0.3 , where such difference in this elastic constant may be responsible for the above noted error of 13 per cent.

A comparison between the maximum interface shear stress reported in Figure 5 (b) of Yao et $al.$ [13] and Figure 5 of this work is presented hereinafter. For an equivalent radius of 2 m, since the head radius is 16 mm, the layer inner radius is 1/(1/16-

1/2000)=16.129 mm, so that the initial radial clearance is 16.129 - 16 = 0.129 mm. A layer thickness of 2 mm, a Young's modulus of 30 MPa and a force of 3000 N are considered. The value of r_i/r_o is therefore 16.129/(16.129+2) = 0.8897 . From Figure 5 of Yao *et al.* [13] the maximum interfacial shear stress is about 1.15 MPa. In addition, p_{ref} = 3000/($\pi \times 16.129^2$) = 3.67 MPa, so that the normalised maximum interface shear stress is 1.15/3.67 = 0.313 . The loading parameter Φ is 3000/(30$\times$16.129$\times$0.129) = 48.05 . For this Φ value, and for r_i/r_o = 0.8897 , Figure 5 of this paper indicates a normalised maximum interface shear stress of 0.332, which closely agrees with the value 0.313 of Yao *et al.* [13], the error being less than 6 per cent.

A final numerical example is presented to clarify further the normalising capabilities of the loading parameter Φ. A mechanical analysis of two different hip replacements, named Case 1 and Case 2 in Table 1, has been carried out with finite elements. The head radius, layer inner and outer radii, radial clearance, layer thickness, Young's modulus, and applied load, are different in the two Cases, but the layer inner to outer radii ratio and the loading parameter Φ are the same. Table 1 fully confirm the analytical expectations according to which, for different hip replacement dimensions, initial clearance and applied load, but for a fixed layer inner to outer radii ratio, the normalised dry contact pressure, the normalised interfacial shear stress, the contact angle, and the angle defining the position of the maximum interface shear stress remain the same for the two Cases 1 and 2 provided that the loading parameter Φ is the same.

Table 1

	Case 1	Case 2
head radius	15.875 mm	17.763 mm
layer inner radius	16.125 mm	18.0 mm
layer outer radius	18.125 mm	20.23 mm
layer inner to outer radii ratio	0.8897	0.8897
initial radial clearance	0.25 mm	0.237 mm
elastomeric layer thickness	2 mm	2.23 mm
Young's modulus	8.506 MPa	5.0 MPa
Poisson's ratio	0.49942	0.49942
applied load	8044 N	5000 N
loading parameter Φ	234.6	234.6
normalised peak contact pressure	2.05	2.05
normalised maximum interface shear stress	0.182	0.182
contact angle	1.27 rad	1.27 rad
angle defining the position of the maximum interface shear stress	0.80 rad	0.80 rad

As an example of the potentials of Φ in the design and optimisation of soft cushion hip replacements, in Wang *et al.* [16]

the wear factor was found to be highly correlated to the maximum contact stress, a parameter which can immediately be extracted from Figure 4 for any applied load, initial clearance, head radius, and Young's modulus, provided that the layer inner to outer radii ratio r_i/r_o falls within the interval 0.8431 - 0.9699.

Geometries have been proposed in which the layer thickness is higher than that covered by the above interval, see *e.g.* Bartel *et al.* [**8**]; such hip replacement geometries would require additional diagrams to be compiled. It may however be noted that "when the thickness is large, the contact stress becomes less sensitive to changes in thickness", Bartel *et al.* [**8**].

A second example illustrating the usefulness of Φ is presented in the following. It is well known that, during walking, the force applied to the head deviates from the direction of the acetabular cup symmetry axis, *e.g.* Unsworth and Strozzi [**11**]. As a consequence of this angular deviation, the undesired situation may occur in which the contact zone reaches the rim of the hemispherical elastomeric cup, thus causing edge loading.

It may be surmised that the diagrams of Figures 4 to 7, compiled for axisymmetric situations, are provisionally applicable even when the force imposed to the head is not axial. This assumption is corroborated by the fact that, in axisymmetric situations, the mechanical responses of a hemispherical elastomeric cup or of a fully spherical cup remain very similar even when the contact zone approaches the rim of the hemispherical cup, Unsworth and Strozzi [**11**].

Within the above approximations, from Figure 6 it is possible to guess if the contact area reaches the layer edge. For instance, if the maximum angular deviation of the applied force from the cup axis is, say, 40°, and if the cup is perfectly hemispherical, the maximum allowed contact angle β preventing the unfavourable circumstance that the contact region reaches the layer rim is 90° − 40° = 50° = 0.8727 rad. If r_i/r_o is 0.9416 , from Figure 6 the value of $\Phi = F/(ER\Delta R)$ corresponding to $\beta = 0.8727$ rad is about 115. If the values of the applied load F, of the Young's modulus E, of the inner radius of the elastomeric layer R, and of the initial radial clearance ΔR, are such that Φ is lower than 115, the contact region will not reach the layer rim. This example shows that Φ accounts for the simultaneous effects of various parameters.

It is finally observed that several normalising parameters have been proposed in connection with the mechanical analysis of soft cushion hip replacements, *e.g.* Strozzi [**10**], Jin *et al*. [**12**], Yao *et al*. [**13**], Strozzi [**6**]. Anyway, no proposed parameter explicitly contains the initial clearance.

4 Application of the loading parameter Φ to metal-on-metal hip replacements

As a result of its normalising and unifying properties, the loading parameter Φ may prove to be fruitful in the mechanical optimisation process of metal-on-metal hip prostheses, characterised by closely conforming mating surfaces, Isaac *et al.* [19].
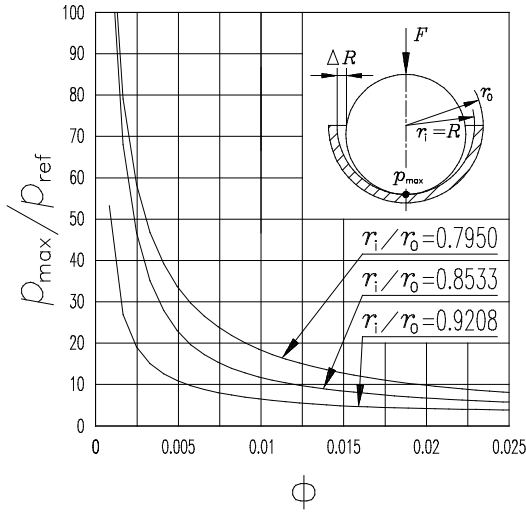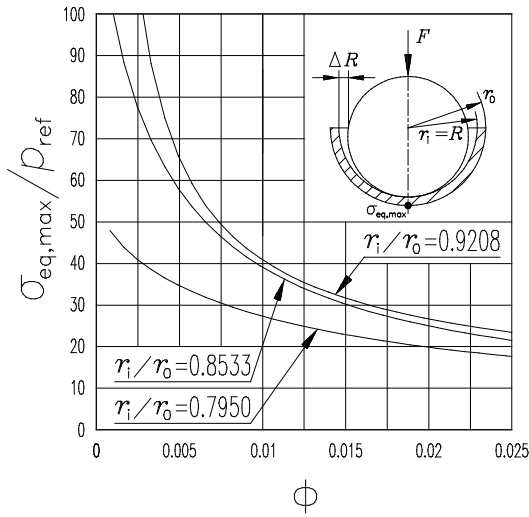

Figure 8

An axisymmetric model has been adopted for compiling the diagrams of Figures 8 to 10, which explore the dependence on Φ of three relevant dry frictionless contact stress parameters: a) the normalised maximum dry contact pressure p_{max}/p_{ref}, see Figure 8; b) the normalised maximum von Mises equivalent stress $\sigma_{eq,max}/p_{ref}$ in the cup, see Figure 9; c) the contact angle β, see Figure 10.

With regard to Figure 8, it is observed that, when the contact extent is small, the maximum contact pressure occurs at the contact centre, as shown in the inset, but for larger contact areas the maximum contact pressure moves laterally, as it appears from Figure 6 of Yew *et al.* [20]. With respect to Figure 9, the maximum equivalent stress often occurs a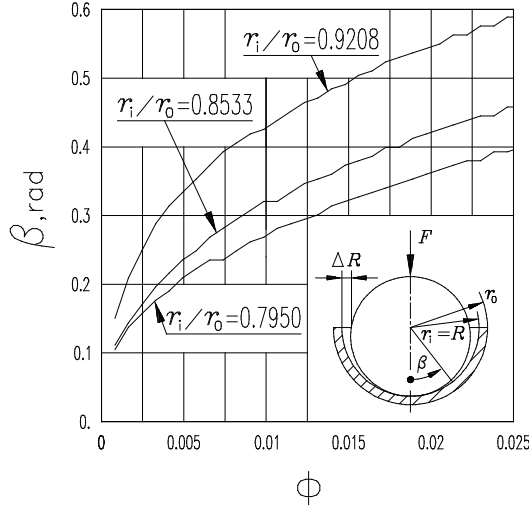t the pole of the cup outer surface, as shown in the inset. Only for very small contact areas the maximum equivalent stress occurs at the centre of the contact zone, just below the contact surface, in agreement with the Hertzian theory.

Figure 9

Figure 10

The finite element model adopted in this study closely follows that of Yew *et al.* [20], and it includes a solid metal head, a metal cup, a layer of cement 6 mm thick, and an axisymmetric model of the pelvic region, where a uniform thickness of 1 mm was assumed for the cortical stratum. The pelvic bone was clamped in a region sufficiently far from the zones of major interest. (The cement layer and the pelvic bone region have not been represented in the insets of Figures 8 to 10.) The elastic constants adopted for the cobalt-chrome alloy, for the cement, and for the cortical and cancellous bones are extracted from Yew *et al.* [20].

As already noted in Section 3, to compile the diagrams reporting the dry contact stress parameters versus Φ, it is convenient to refer to specific dimensions for the hip prosthesis, and to vary the applied load F within a suitable interval. The following dimensions for the metal-on-metal hip replacement have been extracted from Yew *et al.* [20]; the head radius is 17.4385 mm; the radial clearance ΔR is 0.079 mm, so that the cup inner radius r_i is 17.5175 mm; three values of the cup radial thickness have been considered, namely 1.506 , 3.012 , 4.518 mm, which correspond to three outer radii r_o of 19.0235 , 20.5295 , 22.0355 mm, and to three cup inner to outer radii ratios r_i/r_o of 0.9208 , 0.8533 , 0.7950 . The Young's modulus of the cobalt-chrome alloy is 210000 MPa, and the Poisson's ratio is 0.3. The imposed load ramp is similar to that employed in Section 3.

A selected comparison is presented below between the maximum contact pressure and contact angle extracted from in Figure 6 of Yew *et al.* [20], and Figures 8 and 10 of this work. For a head radius of 17.4385 mm, for a cup radial thickness of 4.518 mm, and for an initial radial clearance of 0.079 mm, the cup inner radius r_i is 17.4385+0.079 = 17.5175 mm, whereas the cup outer radius r_o is 17.5175+4.518 = 22.0355 mm. Consequently, r_i/r_o = 17.5175/22.0355 = 0.7950 . The applied load is 2500 N, so that p_{ref} = 2500/($\pi \times 17.5175^2$) = 2.593 MPa. The Young's modulus is 210000

. From Figure 6 of Yew *et al.* [**20**] the peak contact pressure is 56.33 MPa, and the contact angle is 16°≈0.28 rad. The normalised peak contact pressure is therefore 56.33/2.593 = 21.72 .

The loading parameter Φ is 2500/(210000×17.5175×0.079) = 0.0086 . For such Φ value, and for $r_i/r_o = 0.7950$, Figure 8 of this work indicates a normalised peak contact pressure of 21 and a contact angle of 0.255 rad, where such values are in good agreement with those of Yew *et al.* [**20**].

As already noted in Section 3, the loading parameter Φ refers to dry contacts, and it cannot incorporate the lubrication effects. It has, however, been found that in metal-on-metal hip replacements the dry and lubricated pressure profiles remain very similar, *e.g.* Liu *et al.* [**21**].

Aspects that have not been examined in this study include the maximum tensile stress within the cement layer, the modification of the initial clearance due to wear process, and three-dimensional effects, Yew *et al.* [**20**].

5 Conclusions

A normalising loading parameter Φ useful in describing the mechanical response of plane, pin in plate-like contacts, has been extended to axisymmetric, ball in socket-like contacts. This loading parameter Φ is $F/(ER\Delta R)$, where F is the applied load per unit thickness, E the Young's modulus, R the curvature radius of the mating surfaces before deformation, and ΔR the initial radial clearance. Four diagrams summarising mechanically relevant dry frictionless contact parameters in compliant layered artificial hip joints have been compiled with the aid of finite elements. Such diagrams report the normalised peak dry contact pressure, the normalised maximum interfacial shear stress between layer and backing, the contact angle, and the angle defining the position of the maximum interfacial shear stress, versus the loading parameter Φ, for a selection of four inner to outer radii ratios of the elastomeric layer. Similarly, three diagrams addressing metal-on-metal hip replacements have been prepared, which report the normalised peak dry contact pressure, the normalised maximum equivalent stress within the cup, and the contact angle, versus the loading parameter

Φ, for a selection of three inner to outer radii ratios of the acetabular cup. The above values have been assessed versus several literature results. The usefulness of the loading parameter Φ in normalising the effects of initial clearance, head radius, Young's modulus, and applied load has been illustrated with selected examples.

REFERENCES

1 Dundurs, J. and **Stippes, M.** Role of elastic constants in certain contact problems. *ASME J. Appl. Mech.,* 1970, **37**, 965-970.

2 Ciavarella, M., Baldini, A., Barber, J.R. and **Strozzi, A.** Reduced dependence on loading parameters in almost conforming contacts. *Int. J. Mech. Sci.,* 2006, **48**, 917-925.

3 Ciavarella, M., Strozzi, A., Baldini, A., Giacopini, M., Rivasi, S. and **Rosi, R.** On the applicability of the loading parameter Φ in pinned connections with relevant initial clearance. *Applied Mechanics and Materials*, 2006, **5**-**6**, 155-164.

4 Johnson, K.L. *Contact Mechanics*. Cambridge University press, Cambridge, 1985.

5 Ciavarella, M. and **Decuzzi, P.** The state of stress induced by the plane frictionless cylindrical contact. I. The case of elastic similarity. *Int. J. Solids Structures,* 2001, **38**, 4507-4523.

6 Strozzi, A. Analytical modelling of the elastomeric layer in soft layer hip replacements. *Proc. Instn Mech Engnrs, Part H*, *J. Engineering in Medicine*, 2000, **214**, 69-81.

7 Unsworth, A., Roberts, B. and **Thompson, J.** The application of soft layer lubrication to hip prostheses. *J. Bone Jt Surg*, 1981, **63B**, 297.

8 Bartel, D.L., Burstein, A.H., Toda, M.D. and **Edwards, D.L.** The effect of conformity and plastic thickness on contact stresses in metal-backed plastic implants. Biomech. Engng, 1985, **107**, 193-199.

9 Unsworth, A.U., Pearcy, M.J., White, E.F.T. and **White, T.** Soft layer lubrication of artificial hip joints. Proc. IMechE Int. Conf. *Fifty Years on*, 1987, 715-124 (Mechanical Engineering Publications, London).

10 Strozzi, A. Contact stresses in hip replacements. PhD thesis, University of Durham, 1992.

11 Strozzi, A. and **Unsworth, A.** Axisymmetric finite element analysis of hip replacement with an elastomeric layer: the effects of layer thickness. *Proc. Instn Mech Engnrs, Part H, J. Engineering in Medicine*, 1994, **208**, 139-149.

12 Jin, Z.M., Dowson, D. and **Fisher, J.** A parametric analysis of the contact stress in ultra-high molecular weight polyethylene acetabular cups. *Med. Eng. Phys.*, 1994, **16**, 398-405.

13 Yao, J. Q., Parry T. V., Unsworth A. and **Cunningham J. L.** Contact mechanics of soft layer artificial hip joints. Pt.2: Application to joint design. *Proc. Instn Mech Engnrs, Part H, J. Engineering in Medicine*, 1994, **208**, 206-215.

14 Unsworth, A. and **Strozzi, A.** Axisymmetric finite element analysis of hip replacement with an elastomeric layer: the effects of clearance and Poisson's ratio. *Proc. Instn Mech Engnrs, Part H, J. Engineering in Medicine*, 1995, **209**, 59-64.

15 Jin, Z.M. A general axisymmetric contact mechanics model for layered surfaces, with particular reference to artificial hip joint replacements. *Proc. Instn Mech Engnrs, Part H, J. Engineering in Medicine*, 2000, **214**, 425-435.

16 Wang, A., Essner, A. and **Klein, R.** Effect of contact stress on friction and wear of ultra-high molecular weight polyethylene in total hip replacement. *Proc. Instn Mech Engnrs, Part H, J. Engineering in Medicine*, 2001, **215**, 133-139.

17 Prati, E. and **Strozzi, A.** A study of the elastohydrodynamic problem in rectangular elastomeric seals. *ASME J. Tribology*, 1984, **106**, 505-512.

18 Strozzi, A. and **Unsworth, A.** An appraisal of the paper by O'Carrol et al.. *Proc. Instn Mech Engnrs, 1995, Part H, J. Engineering in Medicine*, 1990, **209**, 203-205.

19 Isaac, G.H., Thompson, J., Williams, S. and **Fisher, J.** Metal-on-metal bearings surfaces: materials, manufacture, design, optimization, and alternatives. *Proc. Instn Mech Engnrs, Part H, J. Engineering in Medicine*, 2006, **220**, 119-133.

20 Yew, A., Jagatia, M., Ensaff, H. and **Jin, Z.M.** Analysis of contact mechanics in McKee-Farrar metal-on-metal hip implants. *Proc. Instn Mech Engnrs, Part H, J. Engineering in Medicine*, 2003, **217**, 333-340.

21 Liu, F., Jin, Z.M., Roberts, P. and **Grigoris, P.** Importance of head diameter, clearance, and cup wall thickness in elastohydrodynamic lubrication analysis of metal-on-metal hip resurfacing prostheses. *Proc. Instn Mech Engnrs, Part H, J. Engineering in Medicine*, 2006, **220**, 695-704.